

# Object Permanence Through Audio-Visual Representations

Fanjun Bu<sup>1</sup>, Chien-Ming Huang<sup>1</sup>

**Abstract**—As robots perform manipulation tasks and interact with objects, it is probable that they accidentally drop objects that subsequently bounce out of their visual fields (e.g., due to an inadequate grasp of an unfamiliar object). To enable robots to recover from such errors, we draw upon the concept of *object permanence*—objects remain in existence even when they are not being sensed (e.g., seen) directly. In particular, we developed a multimodal neural network model—using a partial, observed bounce trajectory and the audio resulting from drop impact as its inputs—to predict the full bounce trajectory and the end location of a dropped object. We empirically show that: (1) our multimodal method predicted end locations close in proximity (i.e., within the visual field of the robot’s wrist camera) to the actual locations and (2) the robot was able to retrieve dropped objects by applying minimal vision-based pick-up adjustments. Additionally, we show that our multimodal method outperformed the vision-only and audio-only baselines in retrieving dropped objects. Our results provide insights in enabling object permanence for robots and offer foundations for ensuring robust robot autonomy in task execution.

**Index Terms**—Object Permanence, Object Localization, Trajectory Prediction, Multimodal Neural Network, Error Recovery.

## I. INTRODUCTION

We all drop objects, from car keys to pens or utensils. When an object is dropped and bounces out of sight, people retrieve the object by estimating its landing position. This ability to retrieve objects that are outside of visual fields is based on an understanding of *object permanence* [1]—objects remain in existence even when they may not be visible. As robots increasingly interact with human-made objects, they are bound to drop objects. Drops can be frequent not only due to the challenging nature of robot grasping [2] because of imperfect sensing, complex human-made objects in unstructured human environments, and computationally intensive pose estimations, but also because robots may accidentally drop objects during manipulation. This paper addresses the problem of *how robots may recover from dropping objects*, with a particular focus on how robots may retrieve objects that bounce out of their visual fields by estimating bounce trajectories and object locations (Fig. 1).

Drawing inspiration from humans’ ability to locate objects using multiple sensing modalities, we developed a multimodal deep network that takes as input a partial, observed trajectory and impact sound to predict an object’s bounce trajectory and end location. Our multimodal network encodes modality-specific features from visual and auditory channels and uses observed partial trajectories to adjust audio-driven spatial predictions enabled by a microphone array. To illustrate our multimodal approach to object permanence, we used a simple

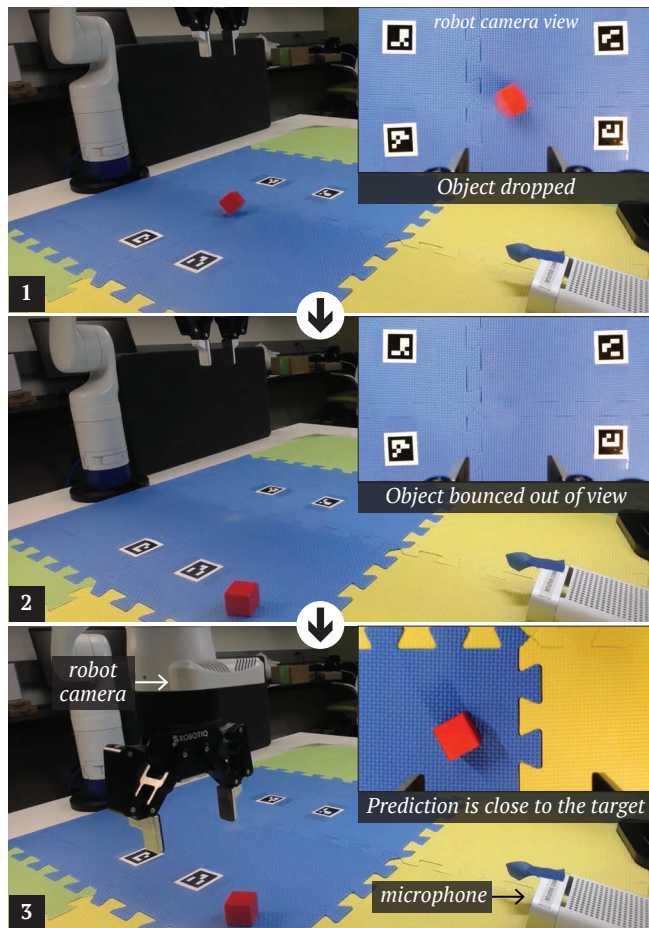


Fig. 1: We explore object permanence through audio-visual representations and contextualize our exploration in a scenario in which a robot seeks to retrieve dropped objects that bounce out of its visual field.

wooden object and compared our approach to unimodal baselines (i.e., vision-only and audio-only). We additionally explored the generalizability of our approach to a different object and dropping height. Our contributions include: (1) a human-inspired multimodal approach to object permanence, (2) a demonstration of how a robotic manipulator may use the multimodal approach to recover from object dropping, and (3) an open dataset of object dropping for the robotics community. Next, we briefly highlight relevant prior research that motivates this work.

## II. BACKGROUND AND RELATED WORK

### A. Object Permanence in Robotics

The concept of object permanence originates from the fields of psychology and child development, and has motivated

<sup>1</sup> {fibu2, chienming.huang}@jhu.edu Department of Computer Science, Johns Hopkins University, Baltimore, MD 21218, USA

research in developmental robotics [3]. Prior research on object permanence in robotics has focused on realizing the concept of object permanence to enable robots to understand the effects of their own actions and facilitate their interactions with people. For example, object permanence has been explored to enable perspective taking and to support situated dialog between humans and robots [4], [5]. It has also been studied as a mechanism for self-monitoring, allowing robots to distinguish self-generated movements from external movements and thus infer the effects of their own actions. Such monitoring mechanisms can help robots form mental representations of objects that were occluded by their own actions [6]–[8]. In contrast to previous research, the present work focuses on investigating how object permanence may be realized by modeling audio-visual inputs and used by a manipulator to retrieve objects that bounce out of its view.

### B. Trajectory Prediction

The problem of trajectory prediction has been widely investigated to enable robot autonomy. For instance, a growing body of research focuses on modeling and predicting pedestrian trajectories to enable mobile robots to navigate in a safe and socially appropriate manner among people (e.g., [9]–[13]). Recent works have also investigated vehicle trajectory prediction in an effort to develop self-driving cars (e.g., [14], [15]). The common property shared by pedestrian trajectories and self-driving car trajectories is that both are goal-oriented. When the trajectories are not driven by intentional agents but purely law of physics, physics-based and dynamics models are commonly used (e.g., [16], [17]). In our work, we focus the prediction of bounce trajectories of dropped objects using modern machine learning approaches with the goal to enhance robot autonomy in events of unintended object dropping.

### C. Audio-Visual Joint Reasoning

Joint reasoning using audio-visual inputs, in general, supports target localization, tracking, and hence navigation (e.g., [18]–[21]). For example, a deep neural network that utilizes both vision and auditory inputs outperforms conventional methods that rely on single modalities in object tracking [18]. Similarly, a simultaneous localization and mapping (SLAM) framework that uses both audio and visual inputs has been shown to localize both human speakers and the observer effectively [19]. A variational expectation-maximization algorithm that takes audio and visual signals as inputs is able to track the location of multiple speakers in the scene [20]. Rather than focusing on tracking, this work focuses on predicting a partially unobservable trajectory that resulted from object dropping using the observed portion of the trajectory and a complete impact sound recording.

## III. PROBLEM STATEMENT

Our goal is to enable robots to recover from inadvertent object dropping. In this work, we consider a robotic manipulator with a wrist camera and that does not rely on external visual sensing capability for error recovery, and we focus on erroneous situations in which objects bounce out of the robot’s visual field. To contextualize our investigation,

we experimentally let the robot drop a wooden block and collected its partial trajectory, as observed through its wrist camera, and the corresponding impact sound due to the dropping. Our primary technical problem is the recovery of the full bounce trajectory given the partial trajectory and impact sound.

## IV. MULTIMODAL NETWORK FOR OBJECT PERMANENCE

We developed a new network architecture<sup>1</sup>, inspired by SELDnet [22], that takes as inputs an observed partial trajectory and a complete audio recording and outputs the object’s bounce trajectory and its end location with respect to the robot. Fig. 2 illustrates our multimodal network.

### A. Feature Extraction

1) *Audio*: Similar to the approaches proposed in SELDnet [22] and DOAnet [23], we extracted magnitude and phase components from spectrograms of each channel of the microphone array. The magnitude and phase components were then stacked along the channel dimension and treated as a  $M/2$  by  $2 \times C$  image, where  $M$  is the window length of the Fourier transformation and  $C$  is the number of channels (Fig. 2). After processing the whole audio sequence with 50% overlap on window size, the shape of the audio data was  $T \times M/2 \times 2C$ , where  $T$  is the number of data points in the time dimension. The parameters used for our feature extraction followed those in SELDnet [22] and DOAnet [23].

2) *Vision*: Observed trajectories were represented as NumPy arrays with shape  $(65, 2)$  after being extracted from series of images using a color tracking algorithm (detailed in Section V).

### B. Audio Feature Encoder Module

As informed by SELDNet [22], we encoded audio features through convolutional recurrent neural networks. To learn inter-channel and intra-channel features across time, we used four 3D convolutional layers with kernel size  $(k, k, c)$  to compute our audio representations.  $(k, k)$  is the kernel size in the time-frequency dimension, which aims to capture correlations within the channel across time;  $c$  is the total number of channels, which allows for finding correlations across all available channels. 3D max pooling layers were added between convolutional layers to reduce the dimension along the frequency axis.

The encoded audio representations were then passed to two layers of bidirectional Gated Recurrent Units (GRUs) (input dimension = 64, hidden dimension = 64, number of layers = 1), seeking to further encode possible connections in the time domain (Fig. 2).

### C. Vision Encoder Module

The vision encoder module is a three-layer multilayer perceptron (MLP) that maps the  $65 \times 2$  partial observed trajectories from the robot’s wrist camera to a higher-dimensional feature vector that matches the shape of the output of the bidirectional GRUs ( $T \times 128$ ).

<sup>1</sup>Our code is available at: <https://intuitivecomputing.jhu.edu/openscience.html>

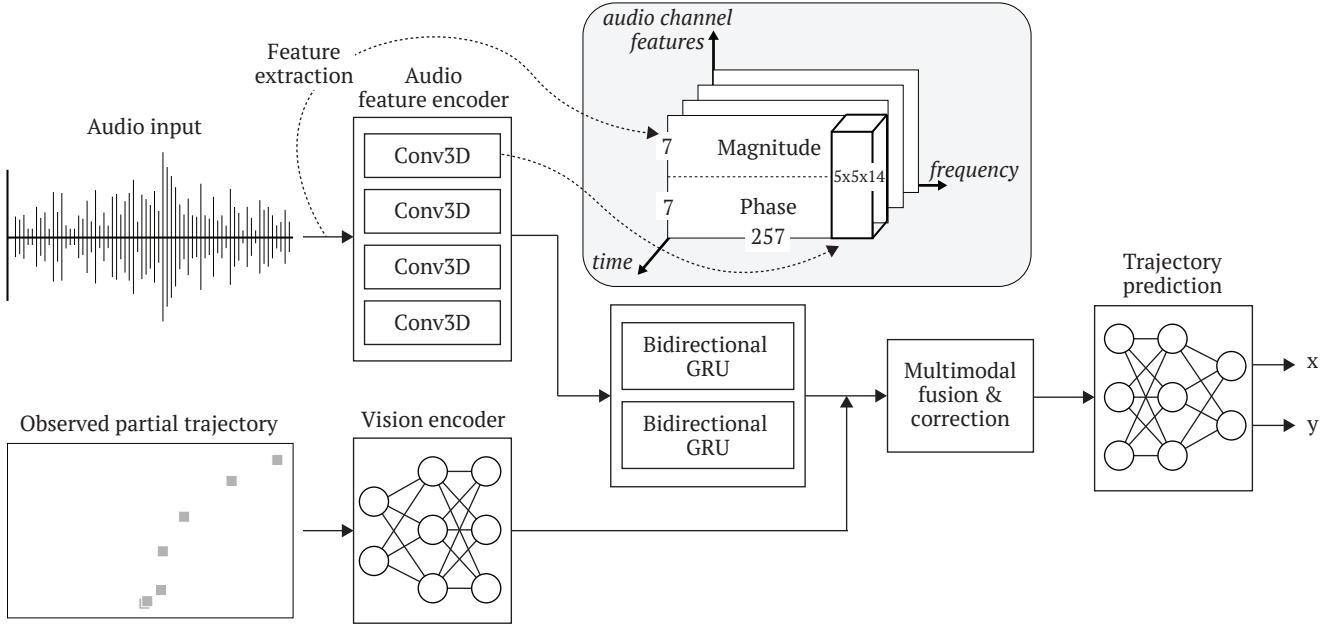


Fig. 2: Structure of our multimodal neural network.

#### D. Multimodal Fusion & Correction Module

The audio representation ( $T \times 128$ ) and the visual feature vector ( $T \times 128$ ) are stacked into one 2D vector ( $T \times 256$ ), which is subsequently fed into a two-layer MLP. The audio representation reflects the complete trajectory, while the visual representation describes the observed, partial trajectory. Consequently, the visual representation serves as a mechanism to provide corrective adjustments to the location information embedded in the audio representation. The output of the fusion and correction module ( $135 \times 256$ ) encodes each  $(x, y)$  coordinate in a 256-dimensional vector, with 135 being the time length for complete trajectories.

#### E. Trajectory Prediction Module

The trajectory prediction module is a three-layer MLP (hidden layer size: (64, 16)) that decodes the 256-dimensional vector representation from each time step and outputs a corresponding  $(x, y)$  location. We note that our prediction includes the full trajectory so as to ensure robustness against missing frames.

### V. EXPERIMENT: OBJECT LOCALIZATION AND TRAJECTORY PREDICTION

In this section, we describe an experiment that sought to evaluate the effectiveness of our multimodal model in predicting the object bounce trajectory and end location based on a partially observed trajectory and impact sound.

#### A. Task and Data Collection Setup

Our experimental task involved a robot picking up a red wooden cube (3 cm x 3 cm x 3 cm) and releasing it from the same height (0.3 meters above the table surface) repeatedly. In all trials, the cube stopped moving within three seconds after release. Our data collection setup is shown in Fig 1. We

used a Kinova Gen3 robot, which has a built-in RGB-D wrist camera (*robot camera*). A Microsoft Azure DK camera was used to collect impact sounds; we note that we only used its embedded microphone array (seven channels; 48k sampling rate). The microphone was positioned to reduce noise from the robot motors. A RealSense D435 camera was mounted on the ceiling (*ceiling camera*) to collect the ground truth videos, which included object trajectories outside of the robot camera’s visual field. Both the robot and ceiling cameras had a data rate of 30 frames per second.

#### B. Experimental Data

1) *Data Collection, Synchronization, and Processing:* In each trial, the robot camera and the ceiling camera published RGB images separately to different ROS topics. To synchronize all of the recording devices (two cameras and a microphone array), two processes were run right before the robot released the object; the first process listened to both ROS topics and saved images in a rosbag file, whereas the second process recorded audio data using the PyAudio package. All processes ran in parallel for three seconds.

To extract object trajectories, we wrote a simple color tracking program using OpenCV [24]. Our goal was to extract the location of the cube in each frame for both cameras. To this end, we defined the range for the color red in HSV space and masked out the contours of red objects. The center of the object contour was recorded to represent the current location of the object.

Each camera, in practice, captured only a portion of the complete trajectory. The robot camera captured the trajectory up to the moment when the cube bounced outside of its visual field (*observed trajectory*). The ceiling camera was initially blocked by the robot gripper and therefore was not able to observe the release of the cube. However, the ceiling

camera was able to keep track of the cube after the cube was outside of the robot camera’s visual field (*post trajectory*). To synchronize coordinate frames between the two cameras, four ChArUco markers were taped onto the table surface such that they were initially visible to both the ceiling camera and the robot camera, allowing the post trajectory to be transformed to the coordinate frame of the robot camera. After this transformation, the overlapping portion between the observed trajectory and the post trajectory was removed from the post trajectory.

We kept the last 65 coordinates recorded in the observed trajectory and the first 70 coordinates recorded in the post trajectory to keep the model input size fixed. The numbers 65 and 70 were chosen based on observation and can be interpreted as the modes of the corresponding trajectory sets’ lengths. If the length of an observed trajectory was greater than 65, the beginning of the observed trajectory could be removed without losing information since the cube was still in the air while the first few coordinates were recorded. If the length of a post trajectory was longer than 70, the last few coordinates could be removed without losing information since the cube always stopped moving during the three-second movement window, leaving the last few data points the same. For similar reasons, if the length of an observed trajectory or a post trajectory were less than 65 or 70, we could prepend or postpend the first or last data point, respectively, to keep the input size of our network fixed.

After the above processing steps, a complete trajectory was formed by concatenating an observed trajectory with its corresponding post trajectory.

2) *Dataset*: A total of 1404 trajectories<sup>2</sup> was included in this experiment. All included data points contained full trajectories from the ceiling camera’s point of view; instances where the experimental cube rolled out of the ceiling camera’s view were excluded. All trajectories were collected with a red wooden cube released from 0.3 meters above the table surface. The complete trajectories from the ceiling camera served as ground truth in this experiment.

Each data point consists of a three second long audio recording and two NumPy 2D arrays that contain the pixel location of the cube in the image frames from the robot camera and the ceiling camera. An observed trajectory from the robot’s wrist camera is a NumPy array with shape (65, 2); a complete trajectory from the ceiling camera is a NumPy array with shape (135, 2). Each row in the trajectories is the  $(x, y)$  coordinate of the object in the image plane.

All trajectories were normalized, and the initial locations of the trajectories were set as the origin using the equation:  $trajectory = trajectory[0] - trajectory$ .

### C. Comparison Baselines

In this experiment, we compared our multimodal method against two unimodal baselines.

1) *Vision Baseline*: Most trajectory prediction models utilize state-of-the-art recurrent neural network architectures. Our vision baseline was motivated by one such architecture: the Social GAN [9], which utilizes long short-term memory (LSTM) [25] in predicting human movement trajectories.

We implemented our vision baseline based on LSTM. First, we embedded each 2D coordinate of the observed trajectory in a 64-dimensional vector. Then, an encoder (implemented using LSTM, input dimension = 64, hidden dimension = 64, number of layers = 1) took the 65 embedding vectors as inputs and outputted its final hidden state. A decoder (implemented using LSTM, input dimension = 64, hidden dimension = 128, number of layers = 1) took the 64-dimensional embedding of the last 2D location coordinate of the observed trajectory and the final hidden state of the encoder as inputs and recursively predicted the difference between consecutive locations sequentially for the 70 unseen trajectory positions, which we normalized. Our choice of parameters was consistent with that in Social GAN [9]. Note that the decoder predicted recursively starting at the end location of the observed trajectory. Thus, we needed to include the observed trajectory in our predicted complete trajectory. This is different from the multimodal model we proposed, where we did not take the observed trajectory as exact in the prediction.

2) *Audio Baseline*: The audio baseline mirrored our multimodal network, except that it did not include the vision input, vision encoder, and fusion components. The audio representation produced by the bidirectional GRUs was passed to the trajectory prediction network directly. Conceptually, this baseline addressed the sound localization problem without vision-based corrective adjustments.

### D. Model Training

We split our 1404 data samples into training, validation, and test sets using an 8:1:1 ratio. We trained all models with the Adam optimizer using a learning rate of  $1e - 4$  and a momentum parameter of 0.9.

### E. Evaluation Metrics

To compare model performance, we employed three evaluation metrics, focusing on whether or not the robot was able to retrieve the dropped objects successfully and on how accurate the predictions were in terms of the end location and trajectory. Below, we describe these metrics in detail.

1) *Task Success Rate*: In practice, the robot is able to reposition itself using a simple vision-based alignment method to retrieve the object when it is in the camera view (Fig. 1). Therefore, we considered a prediction as successful if the dropped object was visible to the robot’s wrist camera when the robot was located at the end of the predicted trajectory. We defined task success rate as the number of trials with a successful prediction divided by the total number of trials.

2) *Target Displacement Error*: Target displacement error represents the distance (in centimeters) between the end location of a predicted bounce trajectory and the ground truth end location.

<sup>2</sup>The full dataset is available at: <https://intuitivecomputing.jhu.edu/openscience.html>

3) *Trajectory Similarity*: To compute the similarity between a predicted trajectory and its corresponding ground truth trajectory, we measured correlations between the two trajectories in both the x- and y- axes. Conceptually, these correlation metrics sought to measure how well the model predicted nonlinear trajectories, as most trajectories were nonlinear (Fig. 3).

## F. Results

Table I summarizes the results of the model performance on the test dataset. Overall, our multimodal network outperformed the unimodal baselines in all metrics, suggesting that the learned multimodal representation captured meaningful location information from both modalities.

Figure 3 shows samples of trajectory predictions. In general, the vision baseline model almost always predicted linear trajectories. It appears that the vision model may have relied on two sources of information that were implicitly contained in the partial observations for prediction: (1) the distance between consecutive observed locations (capturing bounce speed) and (2) directional change in consecutive observed locations. When a bounce trajectory was close to linear, this vision model worked reasonably well (Fig. 3 (e)). However, more often than not, the bounce trajectories were not linear (Fig. 3, (a)–(d)).

The audio baseline model seemed to be able to capture nonlinearity in trajectories better than the vision model. We believe that the audio features extracted from the seven-channel microphone array carried more nuanced information that the 2D visual trajectories did not represent. However, early errors (offsets) propagated through the model and influenced later predictions. As shown in Fig. 3 (d) and (e), the offsets accumulated and caused consequential displacement error in the end.

Our proposed multimodal model was able to utilize information from both modalities effectively. The multimodal structure was based on the audio model and included the partial observed trajectory, which seemed to correctively adjust early prediction offsets and reduce the error propagation. In Fig. 3 (d), the audio baseline model captured the general direction, but the accumulation of early offsets led the predictions away from the ground truth; in contrast, the multimodal model reduced the early offsets and produced more accurate predictions. In Fig. 3 (e), the early prediction errors from the audio input were too significant for the model to recover from (potentially due to noise). On the other hand, the multimodal model was still able to utilize the observed information to reduce the errors from the audio modality.

## G. Additional Exploration

While our goal in this paper is not to develop an omnipotent network that predicts well in every possible scenario, we wanted to explore the generalizability of our multimodal representation. To this end, we collected two additional small datasets of size 100: releasing the original object (cube) from a different height (Dataset H) and releasing a different object from the original height of 0.3 meters (Dataset T).

TABLE I: Evaluation results of the vision, audio, and multimodal models on the test dataset.

	Vision	Audio	Multimodal
Task Success Rate	61.2%	68.2%	<b>79.1%</b>
Target Displacement Error	$9.45 \pm 4.50$	$9.98 \pm 8.36$	<b><math>8.70 \pm 5.78</math></b>
Trajectory Similarity: x axis	0.957	0.906	<b>0.961</b>
Trajectory Similarity: y axis	0.921	0.921	<b>0.941</b>

TABLE II: Evaluation results of the finetuned multimodal models using Dataset H and Dataset T on their respective test datasets.

	Dataset H	Dataset T
Task Success Rate	70.2%	72.0%
Target Displacement Error	$10.4 \pm 5.77$	$11.1 \pm 7.53$
Trajectory Similarity: x axis	0.840	0.863
Trajectory Similarity: y axis	0.832	0.788

Specifically, for Dataset H, the cube was released 5 cm higher than the height used in the original experiment. For Dataset T, we used a triangular wooden block to replace the cube. The triangular block can be thought of as the original cube cut in half along the diagonal. These datasets include novel bounce dynamics that were not represented in the original dataset.

To explore generalizability, we first applied the pre-trained weights for the multimodal model directly on the two new datasets and found that the task success rates were 68.1% and 66.0% for Dataset H and Dataset T, respectively. We then finetuned the multimodal network using Dataset H and Dataset T separately, with a smaller learning rate ( $1e - 5$ ), 0 momentum value, and the same training-validation-test approach (ratio 4:2:4). Table II summarizes the results of the finetuned models' performance on the respective test datasets. These results suggest that a small set of data was sufficient in finetuning our multimodal model to achieve reasonable performance.

## VI. ROBOT DEMONSTRATION

Fig. 1 illustrates a manipulator using our multimodal method to locate and retrieve a dropped object. A full demonstration can be seen in our supplementary video<sup>3</sup>. To allow for retrieval actions, we transformed model predictions in the robot camera frame to the world frame. Though predictions were not perfect, as long as the object was present in the robot's camera view, the robot was able to use a simple vision-based method to reposition itself for object grasping.

## VII. DISCUSSION

Object permanence is crucial for autonomous robots to interact with objects and operate in human environments robustly. In this project, we explore object permanence through

<sup>3</sup><https://youtu.be/Rj-ZZf3r4g8>

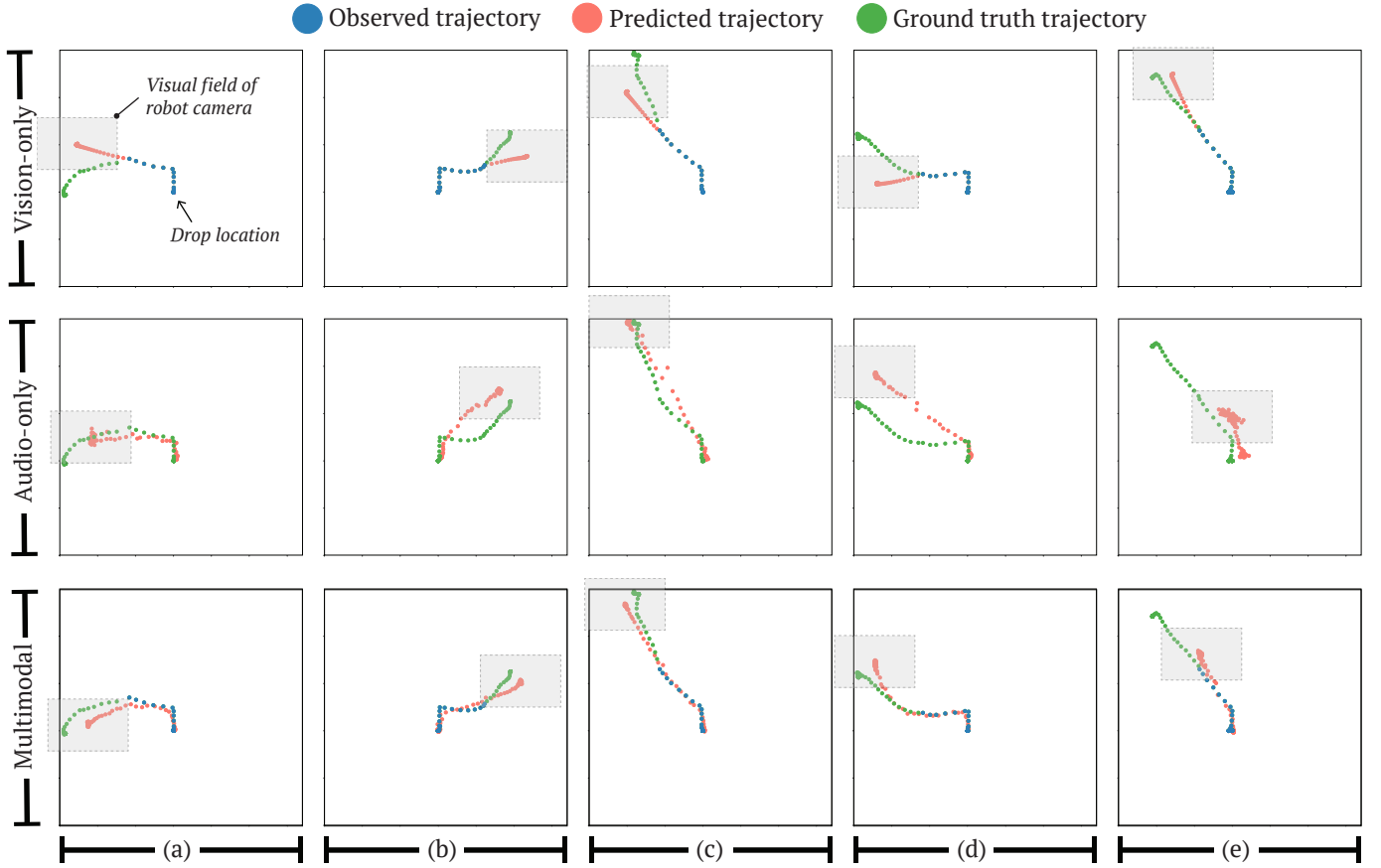


Fig. 3: Sample predictions from the vision, audio, and multimodal models. Each column shows prediction results from the same trial.

object localization and retrieval in the context of dropped objects bouncing out of a robot’s visual field. We developed a multimodal neural network that combines a partial, observed bounce trajectory and the audio resulting from the drop impact to predict the full bounce trajectory and the end location of a dropped object. Our results show that the multimodal network outperformed unimodal methods that only consider vision and audio, respectively.

#### A. Object Permanence for Enhancing Robot Operations

The ability to estimate where dropped objects may be is important in enhancing robot operations. As an example, our multimodal model can be used to let robots recover from accidentally dropping objects efficiently. Rather than relying on external sensing or heuristics-based search, our lightweight model is able to provide reasonable estimations for object retrieval. This ability to estimate object locations also provides robots with a sense of action feasibility. If an object is too far to reach or in a position that the robot cannot find a feasible motion plan to reach, the robot may instead ask for human assistance, minimizing unnecessary grasping attempts. Overall, this ability may be used to foster the fundamental skill of knowing when to ask for help.

#### B. Limitations and Future Work

While showcasing the importance of multimodal representations in understanding of object permanence, this work is not without limitations. The task setup used in this work was experimentally controlled. Future work should explore task settings in natural human environments, diverse dropping scenarios (e.g., accidental drops during robot motions), and a variety of experimental objects (e.g., everyday objects). Future work also needs to explore different audio-visual representations that can encode richer nuances in object properties and physical impact. For instance, both a higher release point and a heavier object can result in an increase in magnitude. In addition to different representations, future work should also consider other sensing modalities that might contribute to the formation of object permanence understanding and, ultimately, the construction of a robot’s mental space. Lastly, more research is need to study object permanence in the context of human-robot collaboration in which objects are jointly used, manipulated, and shared.

#### ACKNOWLEDGMENTS

We would like to thank Gopika Ajaykumar for proofreading this paper and the Johns Hopkins University for supporting this work.

## REFERENCES

- [1] J. Piaget and M. Cook, *The origins of intelligence in children*. International Universities Press New York, 1952, vol. 8, no. 5.
- [2] A. Saxena, J. Driemeyer, and A. Y. Ng, "Robotic grasping of novel objects using vision," *The International Journal of Robotics Research*, vol. 27, no. 2, pp. 157–173, 2008.
- [3] J. Luo, "Rethinking piaget for a developmental robotics of object permanence," in *2007 IEEE 6th International Conference on Development and Learning*. IEEE, 2007, pp. 235–240.
- [4] D. Roy, K.-Y. Hsiao, and N. Mavridis, "Mental imagery for a conversational robot," *IEEE Transactions on Systems, Man, and Cybernetics, Part B (Cybernetics)*, vol. 34, no. 3, pp. 1374–1383, 2004.
- [5] K.-y. Hsiao, N. Mavridis, and D. Roy, "Coupling perception and simulation: Steps towards conversational robotics," in *Proceedings 2003 IEEE/RSJ International Conference on Intelligent Robots and Systems (IROS 2003)(Cat. No. 03CH37453)*, vol. 1. IEEE, 2003, pp. 928–933.
- [6] S. Bechtel, G. Schillaci, and V. V. Hafner, "First steps towards the development of the sense of object permanence in robots," in *2015 Joint IEEE International Conference on Development and Learning and Epigenetic Robotics (ICDL-EpiRob)*. IEEE, 2015, pp. 283–284.
- [7] —, "On the sense of agency and of object permanence in robots," in *2016 Joint IEEE International Conference on Development and Learning and Epigenetic Robotics (ICDL-EpiRob)*. IEEE, 2016, pp. 166–171.
- [8] C. Lang, G. Schillaci, and V. V. Hafner, "A deep convolutional neural network model for sense of agency and object permanence in robots," in *2018 Joint IEEE 8th International Conference on Development and Learning and Epigenetic Robotics (ICDL-EpiRob)*. IEEE, 2018, pp. 257–262.
- [9] A. Gupta, J. Johnson, L. Fei-Fei, S. Savarese, and A. Alahi, "Social gan: Socially acceptable trajectories with generative adversarial networks," in *Proceedings of the IEEE Conference on Computer Vision and Pattern Recognition*, 2018, pp. 2255–2264.
- [10] K. D. Katyal, G. D. Hager, and C.-M. Huang, "Intent-aware pedestrian prediction for adaptive crowd navigation," in *2020 IEEE International Conference on Robotics and Automation (ICRA)*. IEEE, 2020, pp. 3277–3283.
- [11] A. Alahi, K. Goel, V. Ramanathan, A. Robicquet, L. Fei-Fei, and S. Savarese, "Social lstm: Human trajectory prediction in crowded spaces," in *Proceedings of the IEEE conference on computer vision and pattern recognition*, 2016, pp. 961–971.
- [12] Y. Tanaka, J. Kinugawa, Y. Sugahara, and K. Kosuge, "Motion planning with worker's trajectory prediction for assembly task partner robot," in *2012 IEEE/RSJ International Conference on Intelligent Robots and Systems*. IEEE, 2012, pp. 1525–1532.
- [13] A. Rudenko, L. Palmieri, M. Herman, K. M. Kitani, D. M. Gavrila, and K. O. Arras, "Human motion trajectory prediction: A survey," *The International Journal of Robotics Research*, vol. 39, no. 8, pp. 895–935, 2020.
- [14] N. Deo and M. M. Trivedi, "Convolutional social pooling for vehicle trajectory prediction," in *Proceedings of the IEEE Conference on Computer Vision and Pattern Recognition Workshops*, 2018, pp. 1468–1476.
- [15] A. Houenou, P. Bonnifait, V. Cherfaoui, and W. Yao, "Vehicle trajectory prediction based on motion model and maneuver recognition," in *2013 IEEE/RSJ international conference on intelligent robots and systems*. IEEE, 2013, pp. 4363–4369.
- [16] X. Chen, Y. Tian, Q. Huang, W. Zhang, and Z. Yu, "Dynamic model based ball trajectory prediction for a robot ping-pong player," in *2010 IEEE International Conference on Robotics and Biomimetics*. IEEE, 2010, pp. 603–608.
- [17] Y. Huang, D. Xu, M. Tan, and H. Su, "Trajectory prediction of spinning ball for ping-pong player robot," in *2011 IEEE/RSJ International Conference on Intelligent Robots and Systems*. IEEE, 2011, pp. 3434–3439.
- [18] J. Wilson and M. C. Lin, "Avot: Audio-visual object tracking of multiple objects for robotics," 2020.
- [19] A. Chau, K. Sekiguchi, A. A. Nugraha, K. Yoshii, and K. Funakoshi, "Audio-visual slam towards human tracking and human-robot interaction in indoor environments," in *2019 28th IEEE International Conference on Robot and Human Interactive Communication (RO-MAN)*. IEEE, 2019, pp. 1–8.
- [20] Y. Ban, X. Alameda-Pineda, L. Girin, and R. Horaud, "Variational bayesian inference for audio-visual tracking of multiple speakers," *IEEE Transactions on Pattern Analysis and Machine Intelligence*, 2019.
- [21] S. Pleshkova and A. Bekiarski, "Audio visual attention models in the mobile robots navigation," in *New Approaches in Intelligent Image Analysis*. Springer, 2016, pp. 253–294.
- [22] S. Adavanne, A. Politis, and T. Virtanen, "Localization, detection and tracking of multiple moving sound sources with a convolutional recurrent neural network," *arXiv preprint arXiv:1904.12769*, 2019.
- [23] —, "Direction of arrival estimation for multiple sound sources using convolutional recurrent neural network," in *2018 26th European Signal Processing Conference (EUSIPCO)*. IEEE, 2018, pp. 1462–1466.
- [24] G. Bradski, "The OpenCV Library," *Dr. Dobbs's Journal of Software Tools*, 2000.
- [25] S. Hochreiter and J. Schmidhuber, "Long short-term memory," *Neural computation*, vol. 9, no. 8, pp. 1735–1780, 1997.